Computers and Fluids 172 (2018) 301–311

Contents lists available at ScienceDirect

Computers and Fluids

journal homepage: www.elsevier.com/locate/compfluid

Benchmark solutions

Unexpected convergence of lattice Boltzmann schemes☆

Bruce M. Boghosian[a], Francois Dubois[b,c,*], Benjamin Graille[c], Pierre Lallemand[d], Mohamed Mahdi Tekitek[e]

[a] Department of Mathematics, Tufts University, Bromfield-Pearson Hall, Medford, MA 02155, USA
[b] Conservatoire National des Arts et Métiers, Laboratoire de Mécanique des Structures et des Systèmes Couplés, Paris F-75003, France
[c] Department of Mathematics, University Paris-Sud, Orsay Cedex F-91405, France
[d] Beijing Computational Science Research Center, Zhanggguancun Software Park II, Haidian District, Beijing, 100094, China
[e] Department of Mathematics, Faculty of Sciences of Tunis, University of Tunis El Manar, Tunis 2092, Tunisia

ARTICLE INFO

Article history:
Received 6 November 2017
Revised 3 April 2018
Accepted 27 April 2018
Available online 28 April 2018

MSC:
76M28

Keywords:
Heat equation
Damped acoustic
Dispersion equation
Taylor expansion method

ABSTRACT

In this work, we study numerically the convergence of the scalar D2Q9 lattice Boltzmann scheme with multiple relaxation times when the time step is proportional to the space step and tends to zero. We do this by a combination of theory and numerical experiment. The classical formal analysis when all the relaxation parameters are fixed and the time step tends to zero shows that the numerical solution converges to solutions of the heat equation, with a constraint connecting the diffusivity, the space step and the coefficient of relaxation of the momentum. If the diffusivity is fixed and the space step tends to zero, the relaxation parameter for the momentum is very small, causing a discrepancy between the previous analysis and the numerical results. We propose a new analysis of the method for this specific situation of evanescent relaxation, based on the dispersion equation of the lattice Boltzmann scheme. A new asymptotic partial differential equation, the damped acoustic system, is emergent as a result of this formal analysis. Complementary numerical experiments establish the convergence of the scalar D2Q9 lattice Boltzmann scheme with multiple relaxation times and acoustic scaling in this specific case of evanescent relaxation towards the numerical solution of the damped acoustic system.

1. Introduction

Lattice Boltzmann models are simplifications of the continuum Boltzmann equation obtained by discretizing in both physical space and velocity space. The discrete velocities v_i retained typically correspond to lattice vectors of the discrete spatial lattice. That is, each lattice vertex x is linked to a finite number of neighboring vertices by lattice vectors $v_i \Delta t$. A particle distribution f is therefore parameterized by its components in each of the discrete velocities, the vertex x of the spatial lattice, and the discrete time t. A time step of a classical lattice Boltzmann scheme [15] then contains two steps:

(i) A relaxation step where the distribution f at each vertex x is locally modified into a new distribution f^*, and

(ii) an advection step based on the method of characteristics as an exact time-integration operator. We employ the multiple-relaxation-time approach introduced by d'Humières [10], wherein the local mapping $f \longmapsto f^*$ is described by a diagonal operator in a space of moments.

In [6], we have studied the asymptotic expansion of various lattice Boltzmann schemes with multiple-relaxation times for different applications. We used the so-called acoustic scaling, in which the ratio $\lambda \equiv \Delta x / \Delta t$ is kept fixed. We supposed also that the relaxation operator remains fixed. In this manner, we demonstrated the possibility of approximating diffusion processes described by the heat equation.

The importance of using small values of relaxation parameters was recognized for linear viscoelastic fluids by Lallemand et al. [14]. Independently, unexpected results in simulations for advection-diffusion processes have been described by Dellacherie in [4]. We have studied experimentally in [3] the curious convergence of the D1Q3 multiple-relaxation time lattice Boltzmann scheme with one conserved variable when using the acoustic scaling in one spatial dimension. The asymptotic equation of the lattice Boltzmann scheme is no longer an advection-diffusion model but a damped acoustic model. In this contribution, we show and analyze

☆ Contribution to be published in *Computers and Fluids*, edition 31 March 2018.

* Corresponding author at: Department of Mathematics, University Paris-Sud, Orsay Cedex F-91405, France.
E-mail addresses: bruce.boghosian@tufts.edu (B.M. Boghosian), francois.dubois@u-psud.fr (F. Dubois), benjamin.graille@u-psud.fr (B. Graille), pierre.lallemand1@free.fr (P. Lallemand), mohamedmahdi.tekitek@fst.rnu.tn (M.M. Tekitek).

https://doi.org/10.1016/j.compfluid.2018.04.029
0045-7930/

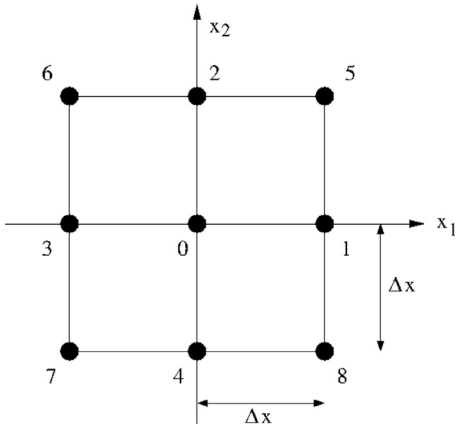

Fig. 1. Particle distribution f_j for $0 \le j \le 8$ of the D2Q9 lattice Boltzmann scheme.

an analogous phenomenon for two spatial dimensions with the scalar D2Q9 lattice Boltzmann scheme. The difficulty concerns the highlighting of the convergence with the numerical experiments.

In Section 2, we recall some fundamentals relative to the D2Q9 lattice Boltzmann scheme for scalar conservation laws. In Section 3, we study convergence of this scheme for diffusive and acoustic scaling. A formal analysis is proposed in Section 4, with the dispersion equation method, initially proposed in [16]. We establish that with acoustic scaling, the convergence of the scalar D2Q9 scheme is not the heat equation but an unexpected model! Finally, we study the experimental convergence of the scalar D2Q9 scheme in several situations in Section 5.

2. Scalar D2Q9 lattice Boltzmann scheme for thermal problems

The D2Q9 lattice Boltzmann scheme uses a set of discrete velocities described in Fig. 1. A density distribution f_j is associated to each velocity $v_j \equiv \lambda e_j$, where $\lambda \equiv \frac{\Delta x}{\Delta t}$ is the fixed numerical lattice velocity. The first three moments for the density and momentum are defined according to

$$\begin{cases} \rho = \sum_{j=0}^{8} f_j = m_0, \\ J_x \equiv \rho u_x = \sum_{j=0}^{8} \lambda e_j^1 f_j = m_1, \\ J_y \equiv \rho u_y = \sum_{j=0}^{8} \lambda e_j^2 f_j = m_2, \end{cases} \tag{1}$$

where the e_j^α are the αth cartesian components of the vectors e_j introduced previously. We complete this set of moments and construct a vector m of moments m_k according to

$$m = Mf, \tag{2}$$

with an invertible fixed matrix M usually [15] given by

$$M = \begin{pmatrix} 1 & 1 & 1 & 1 & 1 & 1 & 1 & 1 & 1 \\ 0 & \lambda & 0 & -\lambda & 0 & \lambda & -\lambda & -\lambda & \lambda \\ 0 & 0 & \lambda & 0 & -\lambda & \lambda & \lambda & -\lambda & -\lambda \\ -4\lambda^2 & -\lambda^2 & -\lambda^2 & -\lambda^2 & -\lambda^2 & 2\lambda^2 & 2\lambda^2 & 2\lambda^2 & 2\lambda^2 \\ 0 & \lambda^2 & -\lambda^2 & \lambda^2 & -\lambda^2 & 0 & 0 & 0 & 0 \\ 0 & 0 & 0 & 0 & 0 & \lambda^2 & -\lambda^2 & \lambda^2 & -\lambda^2 \\ 0 & -2\lambda^3 & 0 & 2\lambda^3 & 0 & \lambda^3 & -\lambda^3 & -\lambda^3 & \lambda^3 \\ 0 & 0 & -2\lambda^3 & 0 & 2\lambda^3 & \lambda^3 & \lambda^3 & -\lambda^3 & -\lambda^3 \\ 4\lambda^4 & -2\lambda^4 & -2\lambda^4 & -2\lambda^4 & -2\lambda^4 & \lambda^4 & \lambda^4 & \lambda^4 & \lambda^4 \end{pmatrix}.$$

For scalar lattice Boltzmann applications, the density ρ is the "conserved variable".

- The particle distribution at equilibrium f^{eq} is a function only of this conserved variable. For this thermal D2Q9 lattice Boltzmann scheme, the vector of equilibrium moments m^{eq} is given by

$$m^{\mathrm{eq}} = \left(\rho, 0, 0, \alpha\lambda^2\rho, 0, 0, 0, 0, \lambda^4\beta\rho\right)^{\mathrm{t}}. \tag{3}$$

In most applications, the coefficients α and β are usually taken to be

$$\alpha = -2, \beta = 1. \tag{4}$$

The lattice Boltzmann scheme is comprised of two fundamental steps : Relaxation and advection. During the relaxation step, the conserved variable ρ is not modified, and the non-conserved moments m_1 to m_8 relax towards an equilibrium value: $m_k^{\mathrm{eq}} = \psi_k(\rho)$ for $k \ge 1$, where the ψ_k are the linear functions of the conserved moment given by (3). The specification of this step also needs relaxation rates s_k : For $k \ge 1$ such that

$$m_k^* = m_k + s_k\left(m_k^{\mathrm{eq}} - m_k\right),$$

where the superscript * denotes the moment m_k after the relaxation step. The table of relaxation parameters s_k chosen in our simulations is as follows

$$[s] = \left(s_J, s_J, s_e, s_x, s_x, s_q, s_q, s_\varepsilon\right). \tag{5}$$

We introduce also the 8×8 diagonal matrix S whose diagonal elements are the components of the vector $[s]$. In our computations, we take the following numerical values

$$s_e = 1.7, s_x = 1.1, s_q = 1.1, s_\varepsilon = 1.7. \tag{6}$$

Only the relaxation coefficient s_J for the first order momentum is allowed to vary in our numerical experiments.

Then using the matrix M^{-1} the relaxation step becomes in f space :

$$f_i^*(x,t) = \sum_\ell M_{i\ell}^{-1} m_\ell^*. \tag{7}$$

During the advection step $f_i(x_j)$ is transported from the node x_j by the discrete velocity v_i to the node $x_j + v_i\Delta t$. Thus the evolution of populations f_i for $0 \le i \le 8$ at internal node x is described by:

$$f_i(x, t+\Delta t) = f_i^*(x - v_i\Delta t, t), 0 \le i \le 8. \tag{8}$$

• In [6], we have analyzed several lattice Boltzmann models with the Taylor-expansion method, including the present one defined by Eqs. (2), (3), (5) and (8). The hypothesis used was that the reference velocity λ and the relaxation coefficients s_J, s_e, s_x, s_q and s_ε remain constant as the spatial step Δx tends to zero. Then the conserved variable ρ satisfies (at least formally!) the heat equation:

$$\frac{\partial\rho}{\partial t} - \kappa\Delta\rho = \mathrm{O}(\Delta x^2), \tag{9}$$

where the thermal diffusivity κ is given by the relation

$$\kappa \equiv \frac{4+\alpha}{6}\sigma\lambda\Delta x, \quad \sigma \equiv \left(\frac{1}{s_J} - \frac{1}{2}\right). \tag{10}$$

The coefficient σ is known as the "Hénon parameter" in reference to the pioneering work of Hénon [9]. Observe that when the relaxation coefficient s_J and the mesh velocity λ are fixed, the thermal diffusivity tends to zero as the space step Δx tends to zero. This lattice Boltzmann scheme is stable in the fluid case (see [15]) under the condition:

$$-4 < \alpha < 2.$$

For the scalar case, the condition $\alpha + 4 > 0$ is clear to assume that the thermal diffusivity κ is positive (see (10)) and the condition $\alpha < 2$ corresponds to our experimental know how. Observe that

with these choices, the value of the relaxation parameter s_J has to be fit with the physical diffusivity κ and the mesh size Δx through the relation (10) if the space step and time step are varying proportionately. In particular, we have the expansion

$$s_J = \frac{4+\alpha}{6\kappa}\lambda\Delta x + O(\Delta x^2) \tag{11}$$

as Δx tends to zero.

• Diffusive scaling can also be used and we refer, e.g., to the work of Junk et al. [11]. In this case, the ratio

$$\frac{(\Delta x)^2}{\Delta t} = \lambda\Delta x$$

remains fixed. This diffusive scaling is intensively used with the explicit finite difference method for solving the heat equation. It is well known [17] that the time step must be proportional to the square of the spacial step in order for the method to be stable. An asymptotic analysis can be done for this simple lattice Boltzmann thermic model, as, e.g., in our contribution [7], and we obtain again the heat Eq. (9) as the scaling limit of the model. With this diffusive scaling, the parameters σ and s_J remain constant if the thermal diffusivity is given and the mesh size Δx tends to zero. Remark also that the convergence of the lattice Boltzmann scheme was rigorously proved for the diffusive scaling for Navier–Stokes flows in periodic and bounded domains in [12] and for one dimensional convection-diffusion-reaction equations in [13].

3. First numerical experiments

We study the diffusion of a Gaussian profile in a square domain. In order to control the computer cost during the numerical experiment and to be certain that the numerical experiment is not polluted by the boundary scheme, we impose periodic boundary conditions. We use two variants of the scalar D2Q9 lattice Boltzmann scheme: Diffusive and acoustic scaling.

• Scalar D2Q9 numerical experiments with diffusive scaling

We solve numerically the heat equation

$$\frac{\partial\rho}{\partial t} - \kappa\Delta\rho = 0, \tag{12}$$

in the square $\Omega = [-1,1]^2$, with periodic boundary conditions. The initial condition is a Gaussian:

$$\rho_0(x,y) = \exp\left(-\frac{x^2+y^2}{0.09}\right), -1 \le x, y \le 1. \tag{13}$$

The coefficients α and β of the equilibrium are fixed according to (4) and we keep fixed the relaxation coefficient for momentum :

$$s_J = \frac{3}{2}. \tag{14}$$

We use the particular diffusive time step $\Delta t = \Delta x^2$. Then $\sigma \equiv \frac{1}{s_J} - \frac{1}{2} = \frac{1}{6}$ and the diffusivity follows the relation $\kappa = \frac{\sigma_J}{3}$ and

$$\kappa = \frac{1}{18}. \tag{15}$$

We have chosen an odd number of mesh cells in these numerical experiments. With the constraint $\Delta t = \Delta x^2$, it is not possible to obtain exactly the same exact final time. We have adapted the number of time steps in order to have very close values for the final time with the different meshes.

• Comparison with finite-difference approximation

Remark that the solution of the heat equation on a square with an initial Gaussian and periodic boundary conditions has to our knowledge no analytical solution. In consequence, we compare the solution obtained by the lattice Boltzmann scheme with the result computed with two-dimensional finite differences, centered in space and explicit in time. The degrees of freedom are located at half-integer positions, exactly as done with the lattice Boltzmann scheme:

$$\rho^n_{i+\frac{1}{2},j+\frac{1}{2}} \approx \rho\left(\left(i+\frac{1}{2}\right)\Delta x, \left(j+\frac{1}{2}\right)\Delta x, n\Delta t\right).$$

We finite difference the heat Eq. (12) in the following way :

$$\begin{cases} \frac{1}{\Delta t}\left(\rho^{n+1}_{i+\frac{1}{2},j+\frac{1}{2}} - \rho^n_{i+\frac{1}{2},j+\frac{1}{2}}\right) \\ \quad -\kappa\left[\frac{1}{\Delta x^2}\left(\rho^n_{i+\frac{3}{2},j+\frac{1}{2}} - 2\rho^n_{i+\frac{1}{2},j+\frac{1}{2}} + \rho^n_{i-\frac{1}{2},j+\frac{1}{2}}\right)\right. \\ \quad\quad \left. + \frac{1}{\Delta y^2}\left(\rho^n_{i+\frac{1}{2},j+\frac{3}{2}} - 2\rho^n_{i+\frac{1}{2},j+\frac{1}{2}} + \rho^n_{i+\frac{1}{2},j-\frac{1}{2}}\right)\right] = 0. \end{cases}$$

We use exactly the same grid in space for both schemes and exactly the same time step (and in consequence the same number of time steps). The parameters for both schemes are compared in Table 1.

The results follow what is expected. The approximate solutions of both schemes are very similar as observed in Figs. 2 and 3 for 111×111 and 223×223 meshes. The difference between the two schemes at the final time is presented in Fig. 4. The order of convergence of this residual is approximately of order 4. Since the finite difference method is of second order accuracy [17], this indicates that the lattice Boltzmann method approaches the heat equation with second-order accuracy.

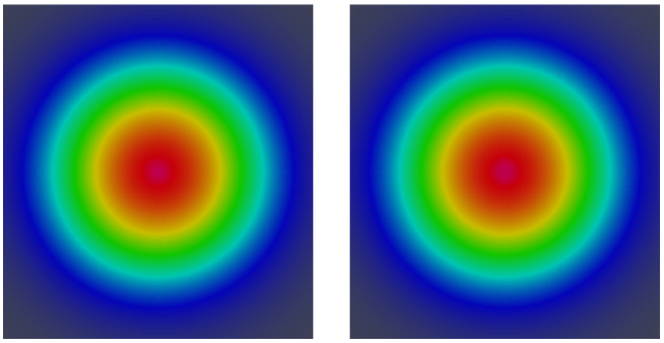

Fig. 2. Two-dimensional heat Eq. (12), $\kappa = \frac{1}{18}$. D2Q9 scheme with diffusive scaling (left) vs. explicit finite differences (right) ; mesh 111×111, time = 0.19479.

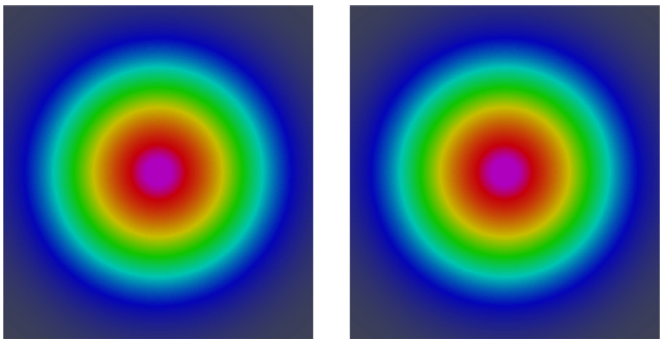

Fig. 3. Two-dimensional heat Eq. (12), $\kappa = \frac{1}{18}$. D2Q9 scheme with diffusive scaling (left) vs. explicit finite differences (right) ; mesh 223×223, time = 0.16473.

Table 1
D2Q9 numerical experiments with diffusive scaling, s_J given by (14) and diffusivity κ by (15).

Number of cells	13×13	27×27	55×55	111×111	223×223
Nb. of time steps D2Q9	8	36	128	600	2048
Final time	0.18935	0.19753	0.17741	0.19479	0.16473

Table 2
D2Q9 numerical experiments with acoustic scaling. The diffusivity $\kappa = \frac{1}{18}$ is imposed in all the simulations.

Number of cells	13×13	27×27	55×55	111×111	223×223
D2Q9 s_J parameter	1.5	1.182	0.830	0.52	0.298
Nb. of time steps D2Q9	8	16	32	64	128
Nb. of time steps, finite differences	8	32	128	512	2048
Final time	0.18935	0.18234	0.17902	0.17741	0.17661

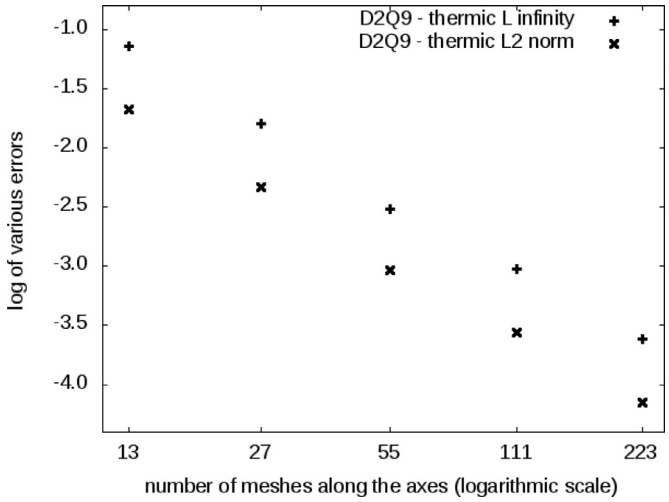

Fig. 4. Two-dimensional heat Eq. (12), $\kappa = \frac{1}{18}$. Difference of the numerical results computed with the D2Q9 scheme with diffusive scaling and explicit finite differences at the final times presented in Table 1. The order of convergence for this residual in the L^∞ norm is equal to 3.41 and in the L^2 norm it is 3.96.

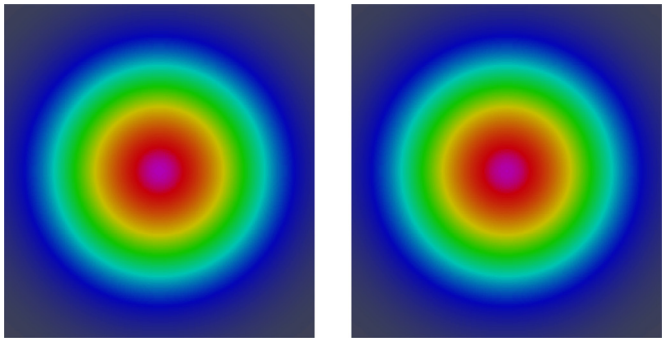

Fig. 5. Two-dimensional heat Eq. (12), $\kappa = \frac{1}{18}$. D2Q9 lattice Boltzmann scheme with acoustic scaling (left) vs. explicit finite differences (right) ; results at time = 0.17741 for a 111 × 111 mesh.

- Scalar D2Q9 numerical experiments with acoustic scaling

We still wish to solve the heat Eq. (12) in the square $\Omega = [-1, 1]^2$ with periodic boundary conditions. The initial condition is again given by a Gaussian profile (13). The given diffusivity is imposed by the value (15). We adopt an acoustic scaling with $\Delta t = \Delta x$ for the D2Q9 lattice Boltzmann simulations. We compare the results with explicit finite differences; in this case, we take $\Delta t \simeq \Delta x^2$ and the time step is chosen in order to obtain exactly the same final time than with the lattice Boltzmann method.

- The numerical results presented in Figs. 5 and 6 for the two meshes of 111×111 and 223×223 seem correct. But a quantitative examination of the results (Fig. 7) shows that after a convergence similar to the one obtained for diffusive scaling (see Fig. 4), a persistent difference appears. This qualitative behavior is very similar to what has been observed in [3] in one spatial dimension.

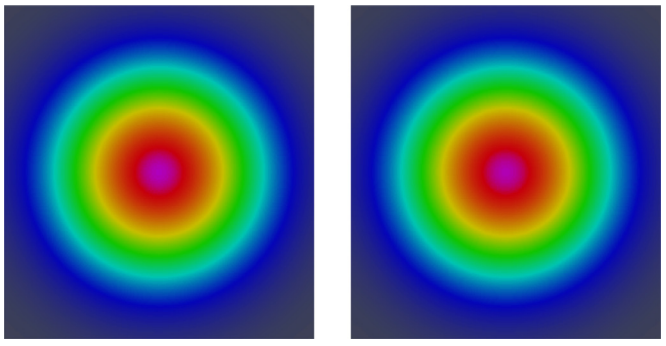

Fig. 6. Two-dimensional heat Eq. (12), $\kappa = \frac{1}{18}$. D2Q9 lattice Boltzmann scheme with acoustic scaling (left) vs. explicit finite differences (right) ; results at time = 0.1766 for a 223 × 223 mesh.

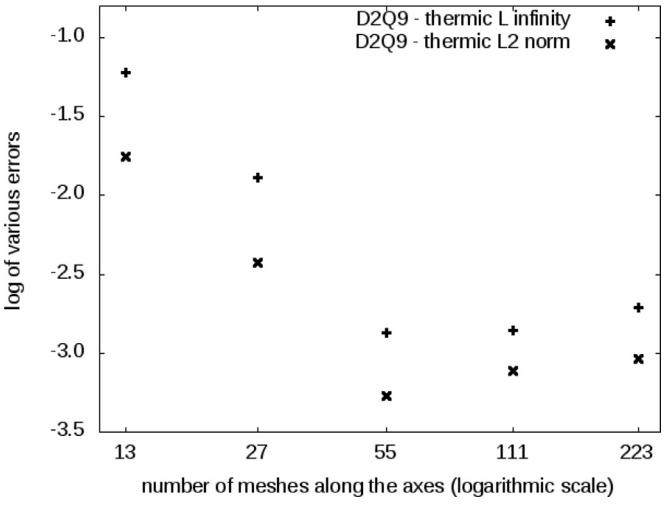

Fig. 7. Two-dimensional heat Eq. (12), $\kappa = \frac{1}{18}$, D2q9 scheme with acoustic scaling vs. explicit finite differences at the final times presented in Table 2. There is no numerical evidence of coherence between the two methods when the mesh is refined.

A new analysis of the scheme is necessary to explain this lack of convergence towards the expected diffusive model.

4. Dispersion equation for an evanescent relaxation

In this section, we propose a first-order analysis when the last relaxation coefficients in (6) remain fixed or when the relaxation coefficient s_J for the momentum J follows the choice presented in Eq. (11), *id est*

$$s_J = \frac{4+\alpha}{6}\lambda^2 \frac{\Delta t}{\kappa} + \mathrm{O}(\Delta t^2). \tag{16}$$

- Fixed relaxations

We write the relation (8) in terms of the moments m defined in (2):

$$m_k(x, t+\Delta t) = \sum_{j\ell} M_{kj} M^{-1}_{j\ell} m^*_\ell (x - v_j \Delta t, t). \tag{17}$$

Before doing a Taylor expansion at order 1, we introduce the following "momentum velocity" operator matrix Λ defined according to

$$\Lambda_{k\ell} \equiv -\sum_{j\ell\alpha} M_{kj} v_j^\alpha M_{j\ell}^{-1} \frac{\partial}{\partial x_\alpha}. \tag{18}$$

For the D2Q9 scheme, this matrix can be explicitly calculated [5] and we have

$$\Lambda = -\left(\begin{array}{c|ccccccccc} 0 & \partial_x & \partial_y & 0 & 0 & 0 & 0 & 0 & 0 \\ \frac{2\lambda^2}{3}\partial_x & 0 & 0 & \frac{1}{6}\partial_x & \frac{1}{2}\partial_x & \partial_y & 0 & 0 & 0 \\ \frac{2\lambda^2}{3}\partial_y & 0 & 0 & \frac{1}{6}\partial_y & -\frac{1}{2}\partial_y & \partial_x & 0 & 0 & 0 \\ 0 & \lambda^2\partial_x & \lambda^2\partial_y & 0 & 0 & 0 & \partial_x & \partial_y & 0 \\ 0 & \frac{\lambda^2}{3}\partial_x & -\frac{\lambda^2}{3}\partial_y & 0 & 0 & 0 & -\frac{1}{3}\partial_x & \frac{1}{3}\partial_y & 0 \\ 0 & \frac{\lambda^2}{3}\partial_y & -\frac{\lambda^2}{3}\partial_x & 0 & 0 & 0 & -\frac{1}{3}\partial_y & \frac{1}{3}\partial_x & 0 \\ 0 & 0 & 0 & \frac{\lambda^2}{3}\partial_x & -\lambda^2\partial_x & \lambda^2\partial_y & 0 & 0 & \frac{1}{3}\partial_x \\ 0 & 0 & 0 & \frac{\lambda^2}{3}\partial_y & \lambda^2\partial_y & \lambda^2\partial_x & 0 & 0 & \frac{1}{3}\partial_y \\ 0 & 0 & 0 & 0 & 0 & 0 & \lambda^2\partial_x & \lambda^2\partial_y & 0 \end{array}\right). \tag{19}$$

We split the moment vector into two blocks:

$$m = \begin{pmatrix} W \\ Y \end{pmatrix} \tag{20}$$

with $W = \rho$ in our scalar example and Y a column vector with 8 components. We decompose also the operator matrix Λ into four blocks that respect the decomposition (20):

$$\Lambda \equiv \begin{pmatrix} A & B \\ C & D \end{pmatrix}. \tag{21}$$

In our case, A is a scalar 1×1 matrix, B has one line and 8 columns, C is composed by 8 lines and 1 column and D is a 8×8 square matrix as shown in the right-hand side of relation (19). We can also introduce a constant matrix E with 8 lines and one column such that the relation (3) can be written in the form

$$Y^{\mathrm{eq}} \equiv Em. \tag{22}$$

The relation (17) is expanded at first order:

$$m + \Delta t\partial_t m + \mathrm{O}(\Delta t^2) = m^* + \Delta t\Lambda m^* + \mathrm{O}(\Delta t^2) \tag{23}$$

and due to (22), we have

$$m^* = \begin{pmatrix} \mathrm{I} & 0 \\ SE & \mathrm{I}-S \end{pmatrix} m. \tag{24}$$

The relation (23) can be written in the form

$$Lm \equiv m^* - m + \Delta t\big(-\partial_t m + \Lambda m^*\big) = \mathrm{O}(\Delta t^2), \tag{25}$$

with

$$L \equiv \begin{pmatrix} 0 & 0 \\ SE & -S \end{pmatrix} + \Delta t\left[\begin{pmatrix} -\partial_t & 0 \\ 0 & -\partial_t \end{pmatrix} + \begin{pmatrix} A & B \\ C & D \end{pmatrix}\begin{pmatrix} \mathrm{I} & 0 \\ SE & \mathrm{I}-S \end{pmatrix}\right]. \tag{26}$$

The dispersion relation associated with the relation (25) can be written in a simple way:

$$\det L = 0. \tag{27}$$

We expand this determinant in order to eliminate the non-conserved moments Y. Moreover, due to the right-hand side of Eq. (25), we can neglect all the terms of second or third order relative to Δt. We write the expression (26) of the matrix L in the form

$$L = \begin{pmatrix} \Delta t(-\partial_t + A + BSE) & \Delta tB(\mathrm{I}-S) \\ SE + \Delta t(C + DSE) & -S + \Delta t(-\partial_t + D(\mathrm{I}-S)) \end{pmatrix}.$$

We apply Gaussian elimination in order to make explicit the condition (27). We multiply this matrix at left by the regular matrix K defined by

$$K = \begin{pmatrix} \mathrm{I} & \Delta tB(\mathrm{I}-S)S^{-1} \\ 0 & \mathrm{I} \end{pmatrix}. \tag{28}$$

Then we have, after some lines of algebra,

$$\begin{aligned} KL &= \begin{pmatrix} \mathrm{I} & \Delta tB(\mathrm{I}-S)S^{-1} \\ 0 & \mathrm{I} \end{pmatrix} \\ &\quad\times \begin{pmatrix} \Delta t(-\partial_t + A + BSE) & \Delta tB(\mathrm{I}-S) \\ SE + \Delta t(C + DSE) & -S + \Delta t(-\partial_t + D(\mathrm{I}-S)) \end{pmatrix} \\ &= \begin{pmatrix} \Delta t(-\partial_t + A + BSE) + \Delta tB(\mathrm{I}-S)S^{-1}SE & \mathrm{O}(\Delta t^2) \\ SE + \mathrm{O}(\Delta t) & -S + \mathrm{O}(\Delta t) \end{pmatrix} \end{aligned}$$

and we have the following triangular form for the product KL:

$$KL = \begin{pmatrix} \Delta t(-\partial_t + A + BE) & \mathrm{O}(\Delta t^2) \\ SE + \mathrm{O}(\Delta t) & -S + \mathrm{O}(\Delta t) \end{pmatrix}.$$

Then the relation (27) is equivalent at first order to the following set of first order partial differential equations:

$$(-\partial_t + A + BE)W = \mathrm{O}(\Delta t), \tag{29}$$

recovering the first step of the Berlin algorithm presented in Augier et al. [2]. For the scalar diffusion problem, this equation expresses simply that

$$\partial_t \rho = \mathrm{O}(\Delta t).$$

This result is consistent with the second-order analysis presented at the relation in (9).

When we use diffusive scaling, this dispersion equation can be adapted in order to recover the heat equation at zero order of accuracy. It is then equivalent to the Taylor expansion method with the diffusive scaling, as used in [7].

- Evanescent relaxations

When Δt and Δx tend to zero with the acoustic scaling, these two infinitesimals are of the same order. The expansion (16) of the relaxation coefficient s_J implies that the previous asymptotic calculus has to be made more precise. The coefficient s_J is now at first order proportional to the time step Δt. We decompose the non-conserved moments Y into two families: The quasi-conserved moments U *id est* the two components of the momentum J in the scalar case– and the other truly non-conserved moments Z:

$$Y = \begin{pmatrix} U \\ Z \end{pmatrix}. \tag{30}$$

The 8-component vector Y is split into a first vector $U \in \mathbb{R}^2$ and a second one Z with 6 components. In other words, the family of moments is split into three components:

$$m = \begin{pmatrix} W \\ U \\ Z \end{pmatrix}.$$

Then the 8×8 relaxation matrix S can be decomposed into two blocks:

$$S = \begin{pmatrix} \Delta t\widetilde{S} + \mathrm{O}(\Delta t^2) & 0 \\ 0 & S_Z \end{pmatrix}. \tag{31}$$

The top left block in the right hand side of (31) tends to zero as the mesh is refined. The equilibrium vector E is naturally split into the quasi-conserved component E_U and the truly relaxing component E_Z:

$$E = \begin{pmatrix} E_U \\ E_Z \end{pmatrix}. \tag{32}$$

We have: $SE = \begin{pmatrix} \Delta t\widetilde{S} & 0 \\ 0 & S_Z \end{pmatrix}\begin{pmatrix} E_U \\ E_Z \end{pmatrix} = \begin{pmatrix} \Delta t\widetilde{S}E_U \\ S_Z E_Z \end{pmatrix}$ and the relation (24) takes the form

$$m^* = \begin{pmatrix} \mathrm{I} & 0 & 0 \\ \Delta t\widetilde{S}E_U & \mathrm{I} - \Delta t\widetilde{S} & 0 \\ S_Z E_Z & 0 & \mathrm{I} - S_Z \end{pmatrix} m. \tag{33}$$

Then the momentum velocity operator matrix Λ is split into 9 blocks:

$$\Lambda = \begin{pmatrix} A & A_2 & B_1 \\ A_3 & A_4 & B_2 \\ C_1 & C_2 & D_4 \end{pmatrix}. \tag{34}$$

This block structure (34) is explicitly given for our thermal D2Q9 in the form

$$\Lambda = \left(\begin{array}{c|cc|ccccccc} 0 & \partial_x & \partial_y & 0 & 0 & 0 & 0 & 0 & 0 \\ \hline \frac{2\lambda^2}{3}\partial_x & 0 & 0 & \frac{1}{6}\partial_x & \frac{1}{2}\partial_x & \partial_y & 0 & 0 & 0 \\ \frac{2\lambda^2}{3}\partial_y & 0 & 0 & \frac{1}{6}\partial_y & -\frac{1}{2}\partial_y & \partial_x & 0 & 0 & 0 \\ \hline 0 & \lambda^2\partial_x & \lambda^2\partial_y & 0 & 0 & 0 & \partial_x & \partial_y & 0 \\ 0 & \frac{\lambda^2}{3}\partial_x & -\frac{\lambda^2}{3}\partial_y & 0 & 0 & 0 & -\frac{1}{3}\partial_x & \frac{1}{3}\partial_y & 0 \\ 0 & \frac{\lambda^2}{3}\partial_y & -\frac{\lambda^2}{3}\partial_x & 0 & 0 & 0 & -\frac{1}{3}\partial_y & \frac{1}{3}\partial_x & 0 \\ 0 & 0 & 0 & \frac{\lambda^2}{3}\partial_x & -\lambda^2\partial_x & \lambda^2\partial_y & 0 & 0 & \frac{1}{3}\partial_x \\ 0 & 0 & 0 & \frac{\lambda^2}{3}\partial_y & \lambda^2\partial_y & \lambda^2\partial_x & 0 & 0 & \frac{1}{3}\partial_y \\ 0 & 0 & 0 & 0 & 0 & 0 & \lambda^2\partial_x & \lambda^2\partial_y & 0 \end{array}\right).$$

Then

$$L = \begin{pmatrix} 0 & 0 & 0 \\ \Delta t\widetilde{S}E_U & -\Delta t\widetilde{S} & 0 \\ S_Z E_Z & 0 & -S_Z \end{pmatrix} - \Delta t\begin{pmatrix} \partial_t & 0 & 0 \\ 0 & \partial_t & 0 \\ 0 & 0 & \partial_t \end{pmatrix} + \Delta t\begin{pmatrix} A & A_2 & B_1 \\ A_3 & A_4 & B_2 \\ C_1 & C_2 & D_4 \end{pmatrix}\begin{pmatrix} \mathrm{I} & 0 & 0 \\ \Delta t\widetilde{S}E_U & \mathrm{I} - \Delta t\widetilde{S} & 0 \\ S_Z E_Z & 0 & \mathrm{I} - S_Z \end{pmatrix}.$$

This expression can be expanded to first order in Δt without any change in the result of the Gaussian elimination. Then we can neglect the terms of order one in Δt in the last product of two matrices. We obtain

$$\begin{pmatrix} A & A_2 & B_1 \\ A_3 & A_4 & B_2 \\ C_1 & C_2 & D_4 \end{pmatrix}\begin{pmatrix} \mathrm{I} & 0 & 0 \\ 0 & \mathrm{I} & 0 \\ S_Z E_Z & 0 & \mathrm{I} - S_Z \end{pmatrix} = \begin{pmatrix} A + B_1 S_Z E_Z & A_2 & B_1(\mathrm{I} - S_Z) \\ A_3 + B_2 S_Z E_Z & A_4 & B_2(\mathrm{I} - S_Z) \\ C_1 + D_4 S_Z E_Z & C_2 & D_4(\mathrm{I} - S_Z) \end{pmatrix},$$

and, up to order $\mathrm{O}(\Delta t)$, we have

$$L = \begin{pmatrix} \Delta t(-\partial_t + A + B_1 S_Z E_Z) & \Delta t A_2 & \Delta t B_1(\mathrm{I} - S_Z) \\ \Delta t(\widetilde{S}E_U + A_3 + B_2 S_Z E_Z) & \Delta t(-\widetilde{S} - \partial_t + A_4) & \Delta t B_2(\mathrm{I} - S_Z) \\ S_Z E_Z + \Delta t(C_1 + D_4 S_Z E_Z) & \Delta t C_2 & -S_Z + \Delta t(-\partial_t + D_4(\mathrm{I} - S_Z)) \end{pmatrix}. \tag{35}$$

With the method of Gaussian elimination used previously, we multiply the matrix L obtained in (35) on the left by the following matrix

$$K' = \begin{pmatrix} \mathrm{I} & 0 & \Delta t B_1(\mathrm{I} - S_Z)S_Z^{-1} \\ 0 & \mathrm{I} & \Delta t B_2(\mathrm{I} - S_Z)S_Z^{-1} \\ 0 & 0 & \mathrm{I} \end{pmatrix}$$

whose determinant is equal to 1. After some elementary algebra, we obtain

$$K'L = \begin{pmatrix} \Delta t(-\partial_t + A + B_1 E_Z) & \Delta t A_2 & \mathrm{O}(\Delta t^2) \\ \Delta t(\widetilde{S}E_U + A_3 + B_2 E_Z) & \Delta t(-\widetilde{S} - \partial_t + A_4) & \mathrm{O}(\Delta t^2) \\ S_Z E_Z + \mathrm{O}(\Delta t) & \Delta t C_2 & -S_Z + \mathrm{O}(\Delta t) \end{pmatrix}.$$

On one hand, $\det K' = 1$ and on the other hand, the last column of the matrix $K'L$ is composed of negligible terms except for the last one. Then we have the condition (27) if and only if the determinant of the 2×2 upper block matrix is null. In other terms, this matrix has a nontrivial kernel at order one relative to Δt and we have

$$\begin{pmatrix} -\partial_t + A + B_1 E_Z & A_2 \\ \widetilde{S}E_U + A_3 + B_2 E_Z & -\partial_t - \widetilde{S} + A_4 \end{pmatrix}\begin{pmatrix} W \\ U \end{pmatrix} = \mathrm{O}(\Delta t). \tag{36}$$

Then the equivalent partial differential equations are written as a system involving the conserved variable W and the quasi conserved moments U:

$$\begin{cases} \partial_t W = (A + B_1 E_Z)W + A_2 U + \mathrm{O}(\Delta t) \\ \partial_t U + \widetilde{S}U = (A_3 + B_2 E_Z + \widetilde{S}E_U)W + A_4 U + \mathrm{O}(\Delta t). \end{cases} \tag{37}$$

This result generalizes the first analysis done in [3] for the D1Q3 scheme. When we replace the block matrices introduced in the relations (31), (32) and (34) by their D2Q9 values, we establish that with the acoustic scaling, the scalar D2Q9 lattice Boltzmann scheme with acoustic scaling admits the following asymptotic damped acoustic model

$$\begin{cases} \dfrac{\partial \rho}{\partial t} + \mathrm{div} J = \mathrm{O}(\Delta x) \\ \dfrac{\partial J_\alpha}{\partial t} + c_0^2 \dfrac{\partial \rho}{\partial x_\alpha} + g J_\alpha = \mathrm{O}(\Delta x), 1 \le \alpha \le 2, \end{cases} \tag{38}$$

with a sound velocity c_0 and a damping coefficient g given by the relations

$$c_0^2 = \frac{\lambda^2}{6}(4 + \alpha), \quad g = \frac{c_0^2}{\kappa}. \tag{39}$$

The above is a very interesting analysis, and clearly the correct two-dimensional analog of the earlier result for D1Q3. We point out that it is equivalent to a damped wave equation.

5. Scalar D2Q9 scheme converging towards damped acoustic

We have now two partial differential equations with which to compare the numerical solution obtained with the scalar D2Q9 lattice Boltzmann scheme: The initial heat Eq. (12) and the damped acoustic system (38). We first consider numerical experiments done in Section 3 and compare our previous results with this new model. We also study in detail the eigenmodes of the system (38) and propose a simple numerical experiment with a sinusoidal analytic solution. The evolution of an initial Gaussian is again performed, with two diffusion coefficients varying by one order of magnitude.

- Damped acoustics as a limiting model for the previous numerical experiments?

We wish to approximate the system of damped acoustic Eqs. (38). The sound velocity is given by (39). With the choice (4), we obtain the classical value $c_0 = \frac{\lambda}{\sqrt{3}}$. The imposed diffusivity κ and the relation (39) fix the value $g = 6$ for the zero-order damping in the momentum equation of (38). The geometry is the square $\Omega = [-1, 1]^2$ with periodic boundary conditions. The initial density is still given by a Gaussian profile (13). Because the momentum J at equilibrium is identically null, we have taken this specific value as initial condition of our lattice Boltzmann simulations. We suppose in consequence that the initial condition for the momentum is simply $J(x, t = 0) = 0$.

We adopt acoustic scaling with $\Delta t = \Delta x$ for the D2Q9 lattice Boltzmann simulations. For the acoustic system (38), we use explicit finite differences with staggered grids, hereafter named as "HaWAY" method and described with some details in the Appendix. In this case, the acoustic time step Δt_a for finite-difference

Table 3
Numerical experiments with the D2Q9 lattice Boltzmann test case studied in Section 3 compared with the damped acoustic model (38) simulated with the HaWAY method.

Number of cells	13 × 13	27 × 27	55 × 55	111 × 111	223 × 223
D2Q9 s_J parameter	1.5	1.182	0.830	0.52	0.298
Nb. of time steps d2q9	8	16	32	64	128
Idem, finite differences	32	64	128	256	512
Final time	0.18935	0.18234	0.17902	0.17741	0.17661

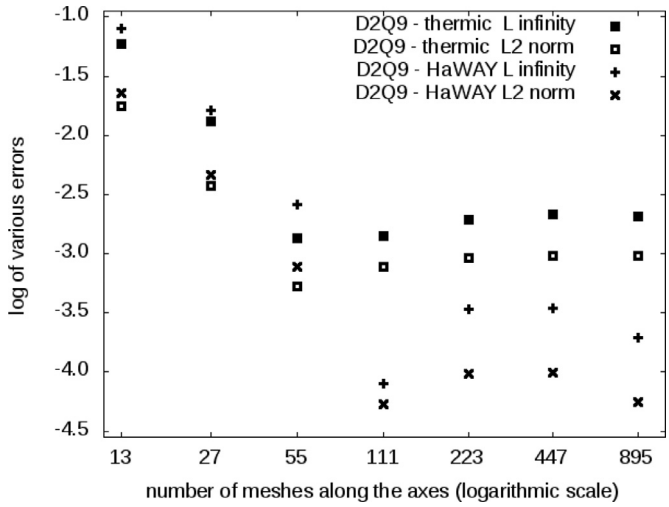

Fig. 8. Numerical results for the damped acoustic model with the experimental plan proposed in Table 3.

Fig. 9. Two-dimensional wave with wave vector $k = 2\pi(1, 1)$. Initial condition.

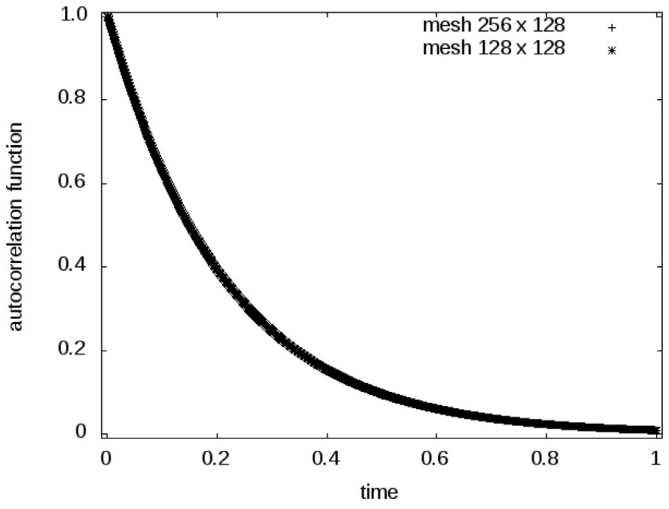

Fig. 10. Two-dimensional wave with wave vector $k = 2\pi(1, 1)$, $g \simeq 6$, $2|k|c_0 \simeq 5.924$. Autocorrelation of density.

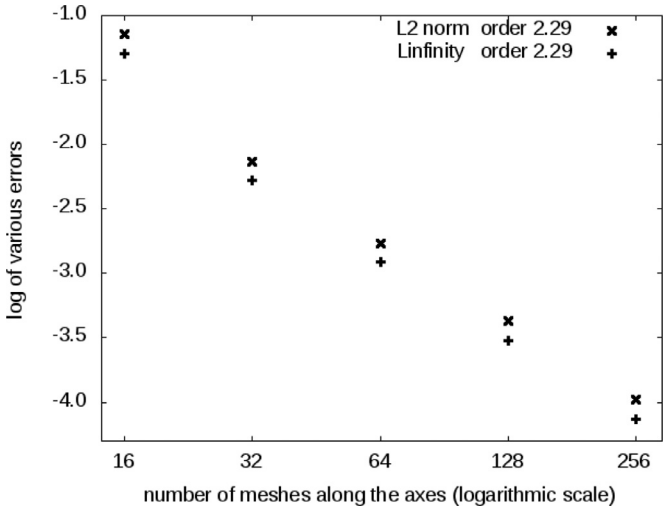

Fig. 11. Two-dimensional wave with wave vector $k = 2\pi(1, 1)$, $g \simeq 6$, $2|k|c_0 \simeq 5.924$. Convergence towards the damped acoustic model (38).

simulations is proportional to the spatial step Δx, with a stability constraint. The corresponding experiments are described in Table 3.

The results obtained with this new experiment are very similar to the one obtained in Section 3. In particular, the numerical results computed with the damped acoustic model are very close to the ones presented in Figs. 5 and 6. When we look to the convergence with quite fine grids (Fig. 8), the signal is better than in Fig. 7 but this experiment is still not entirely convincing.

- Waves for the damped acoustic model

We search modes of the type

$$\begin{cases} \rho = \rho_0 \exp(-\gamma t + ik \cdot x) \\ J = J_0 \exp(-\gamma t + ik \cdot x) \end{cases} \tag{40}$$

for the damped acoustic model 38–(39). Then we have to solve the following ill-posed linear system:

$$-\gamma \rho_0 + ik \cdot J_0 = 0, \quad ik \cdot \rho_0 + (g - \gamma) J_0 = 0. \tag{41}$$

A first solution is a transverse stationary wave with $\gamma = g$, $\rho_0 = 0$ and $k \cdot J_0 = 0$. We do not consider this mode in this contribution. Then the other modes satisfy the following dispersion relation

$$\gamma^2 - g\gamma + |k|^2 c_0^2 = 0. \tag{42}$$

This equation has complex propagative roots when

$$g < 2|k|c_0, \tag{43}$$

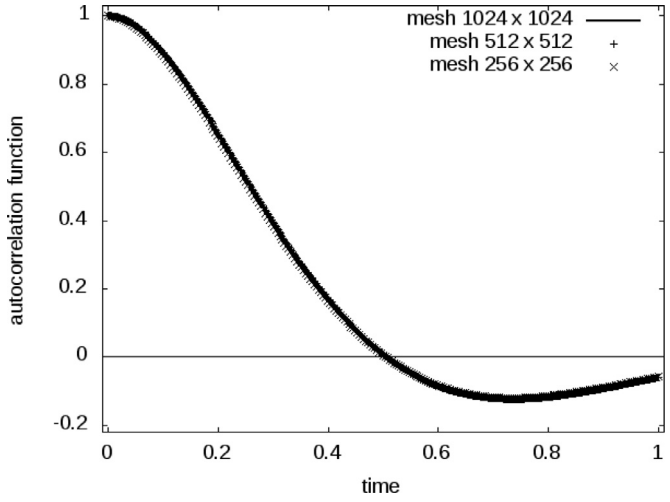

Fig. 12. Two-dimensional wave with wave vector $k = 2\pi(1,1)$, $g \simeq 5.6470$. Autocorrelation of density with $2|k|c_0 \simeq 5.924$ for various meshes.

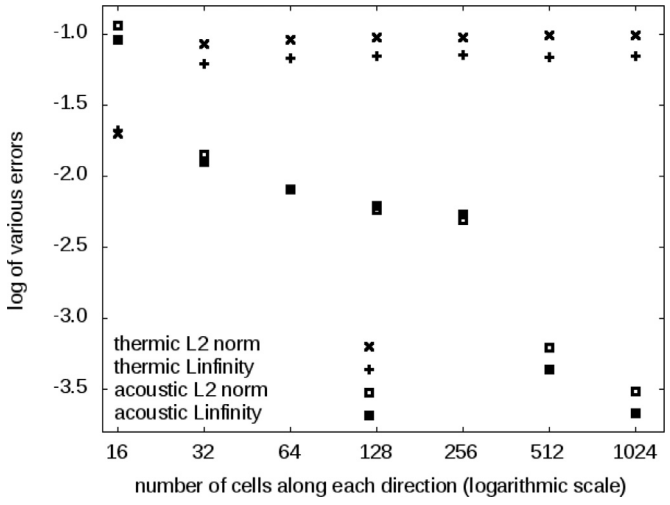

Fig. 13. Two-dimensional wave with vector $k = 2\pi(1,1)$, $g \simeq 5.6470$. Convergence towards the damped acoustic model (38) with $2|k|c_0 \simeq 5.924$. The order of convergence is 1.27 for the L^2 norm and 1.30 in norm L^∞.

i.e., when the diffusivity κ is sufficiently large measured in a scale system based on the sound velocity and wave number:

$$\kappa > \frac{c_0}{2|k|}.$$

In that case, the eigenvalue γ takes the form

$$\gamma = \frac{g}{2} \mp i\omega, \quad \omega = \sqrt{|k|^2 c_0^2 - \frac{g^2}{4}}. \tag{44}$$

The eigenvectors are finally given according to

$$\begin{cases} \rho = \rho_0 \exp\Big(-\frac{g}{2}t\Big)\exp\big(i(k\cdot x \pm \omega t)\big) \\ J = i\frac{k}{|k|^2}\rho_0\Big(-\frac{g}{2} \mp i\omega\Big)\exp\Big(-\frac{g}{2}t\Big)\exp\big(i(k\cdot x \pm \omega t)\big). \end{cases} \tag{45}$$

We consider a pure analytical test case as the next experiment.

- A two-dimensional sinusoidal wave

We keep the value $\kappa = \frac{1}{18} \simeq 0.05555$ of the diffusivity introduced in (15). We use the traditional value $c_0 = \frac{1}{\sqrt{3}}$ and the dissipation coefficient g (see (39)) is still equal to $g = 6$. We change the domain and consider $[0, 2\pi]^2$ with the initial condition $\rho = \cos\big((2\pi(x+y)\big)$ and $J = 0$. Then $k = 2\pi(1,1)$ and the right-hand side of (43) is $2|k|c_0 \simeq 5.924$. In this case, the damped acoustic model (38) exhibits a non-propagative mode.

The initial condition is presented in Fig. 9. The autocorrelation of density

$$\Gamma(t) \equiv \frac{\int_\Omega \rho(x,t)\rho(x,0)\mathrm{d}x}{\int_\Omega |\rho(x,0)|^2 \mathrm{d}x}$$

is typical of a diffusion process as shown in Fig. 10. The convergence for simple dyadic meshes is presented in Fig. 11.

A second numerical experiment has been conducted. We keep the same domain $[0, 2\pi]^2$ with the same initial condition $\rho = \cos\big((2\pi(x+y)\big)$. Then $k = 2\pi(1,1)$ and the right-hand side of (43) is equal to $2|k|c_0 \simeq 5.924$. We change the value of the diffusivity κ introduced in (15) to $\kappa = \frac{17}{288} \simeq 0.05903$. We keep the traditional value $c_0 = \frac{1}{\sqrt{3}}$. Then the dissipation coefficient g (see (39)) is now $g \simeq 5.6470$. Then the damped acoustic model (38) exhibits a propagative mode in this case. The autocorrelation function is presented in Fig. 12. The convergence curve is depicted in Fig. 13. We observe that this convergence is not regular. An extra-fine mesh with dimensions 1024×1024 has been necessary in order to confirm the order of accuracy.

- Complementary experiments for an initial Gaussian

We have compared the scalar D2Q9 lattice Boltzmann scheme with acoustic scaling with numerical solutions of the heat Eq. (12) as presented in Section 3 and with HaWAY simulations of the damped acoustic system (38) in Section 4. We consider again the first geometry studied in this contribution, *id est* the square $\Omega = [-1,1]^2$ with periodic boundary conditions. An initial Gaussian profile (13) is given at $t = 0$. Two numerical experiments have been considered: A quite viscous one with imposed diffusivity $\kappa = 0.15$ and another one with $\kappa = 0.015$. The numerical parameters are displayed in Table 4.

The results for the first test case with $\kappa = 0.15$ are presented in Figs. 14–17. In Fig. 14, a qualitative view of the numerical result on a given mesh shows that the scalar D2Q9 scheme and the HaWAY scheme for damped acoustic are closer to each other than they are to the solution of the heat equation. The three profiles of density are shown in Fig. 15 and a comparison of autocorrelation functions in Fig. 16. Even on a relatively coarse mesh, the conclusion is the same and our new asymptotic analysis of the acoustic system (38) is consistent with the numerical results. Last but not least, both the error between D2Q9 and thermics on one hand, and that between D2Q9 and damped acoustics on the other hand are displayed in Fig. 17. The error between the lattice Boltzmann scheme and the damped acoustic results tends to zero whereas the error between D2Q9 and the thermic model remains stationary.

The second numerical experiment with $\kappa = 0.015$ is presented in Figs. 18–20. At time $= 2$ on a relatively coarse mesh, the three numerical solutions can not be distinguished as shown in Fig. 18. It is also the case for the autocorrelation function as presented in Fig. 19. The numerical convergence is delicate for this test case. During one decade of mesh refinement, the three methods present very close results as shown in Fig. 20. Two additional computations on 895×895 and 1791×1791 refined meshes have been necessary to demonstrate the convergence of the scalar D2Q9 scheme towards the damped acoustic system. Observe that the most refined mesh contains more than 3 millions cells!

6. Conclusion

We have first considered the scalar D2Q9 lattice Boltzmann scheme with diffusive scaling. Our experiments confirm numeri-

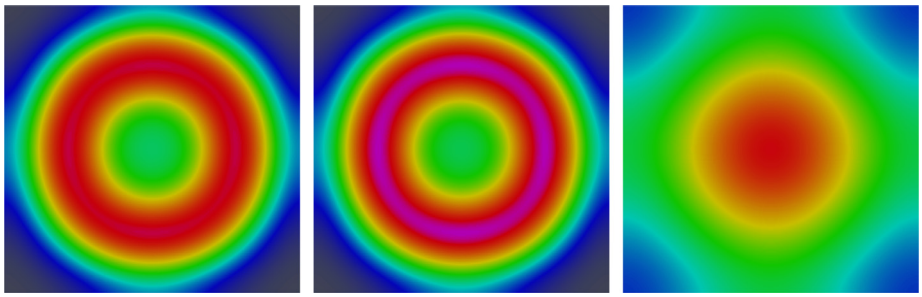

Fig. 14. Initial Gaussian, $\kappa = 0.15$. Three simulations done for the damped acoustic model with finite differences HaWAY discretization (left), D2Q9 lattice Boltzmann scheme (middle), and for the heat equation with finite differences (right). Approximate solutions are presented for time $T = 1$ with 111×111 meshes.

Table 4
Initial Gaussian. D2Q9 numerical experiments with acoustic scaling ; values of s_J for the viscosities $\kappa = 0.15$ and $\kappa = 0.015$.

Number of cells	13^2	27^2	55^2	111^2	223^2	447^2	895^2	1791^2
s_J with $\kappa = 0.15$	0.292	0.152	0.0777	0.0392	0.0197	0.00989		
s_J with $\kappa = 0.015$	1.262	0.903	0.575	0.333	0.181	0.0947	0.0484	0.0245

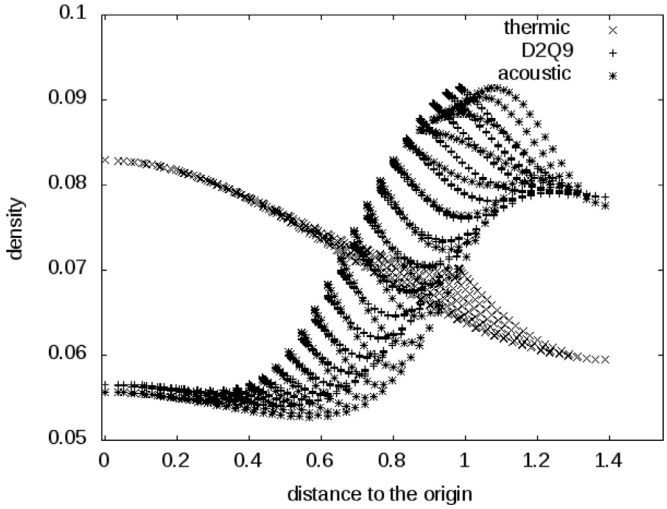

Fig. 15. Initial Gaussian, $\kappa = 0.15$. Three simulations done for the damped acoustic model with finite differences HaWAY discretization, D2Q9 lattice Boltzmann scheme and heat equation with finite differences. Density field at time $= 2$ of a 55×55 mesh.

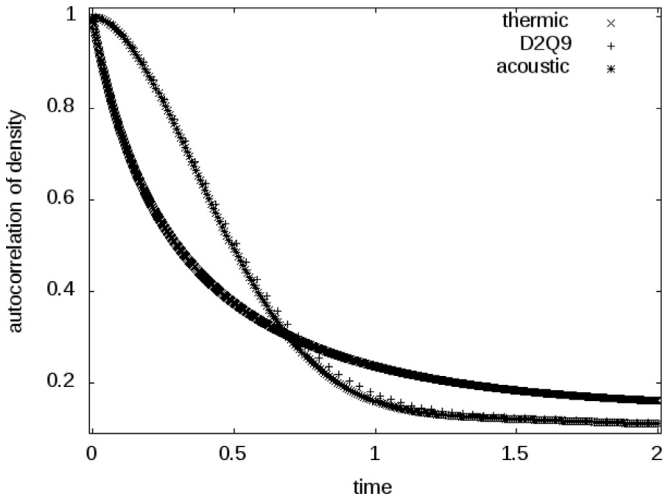

Fig. 16. Initial Gaussian, $\kappa = 0.15$. Three simulations done for the damped acoustic model with finite differences HaWAY discretization, D2Q9 lattice Boltzmann scheme and heat equation with finite differences. Autocorrelation of density for a 55×55 mesh.

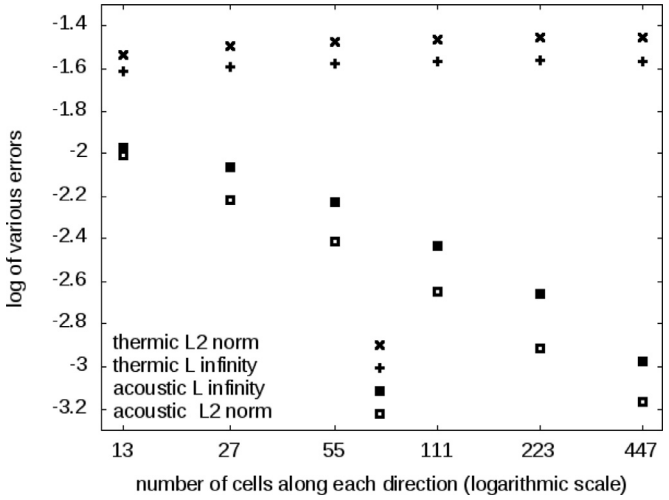

Fig. 17. Initial Gaussian, $\kappa = 0.15$. Damped acoustic model with HaWAY finite differences, D2Q9 lattice Boltzmann scheme and heat equation. The order of convergence at time $= 2$ towards damped acoustic is 0.756 for the L^2 norm and 0.653 in norm L^∞.

cal convergence to the solution of the heat equation. Of course, the mathematical proof of this numerical fact has now to be established.

We have also studied convergence properties of the scalar D2Q9 scheme with an acoustic scaling for the diffusion of a Gaussian profile, when it is supposed to approximate diffusion problems. Our numerical experiments show consistent results with the diffusion equation solution for relaxation parameters that are not too small, $s_J \geq 0.5$ typically. When this relaxation coefficient is very small, however, numerical convergence is defective for the diffusion of a Gaussian.

For very small values of the relaxation parameter, the asymptotic analysis has been revised when the physical diffusion is given. We have developed a new analysis of the lattice Boltzmann method using the dispersion equation and Gaussian elimination when relaxation parameters can tend to zero. This asymptotic analysis shows that a damped acoustic model is emergent at first order. Complementary numerical experiments (see Figs. 11, 13, 17 and 20) show the numerical convergence of the D2Q9 lattice Boltzmann scheme with acoustic scaling and a relaxation coefficient s_J deter-

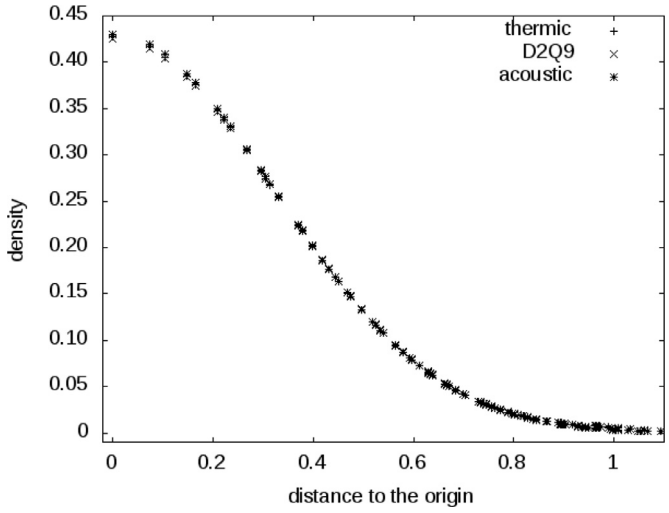

Fig. 18. Initial Gaussian, $\kappa = 0.015$. Three simulations done for the damped acoustic model with finite differences HaWAY discretization, D2Q9 lattice Boltzmann scheme and for the heat equation with finite differences. Density field at time = 2 for a 27×27 mesh.

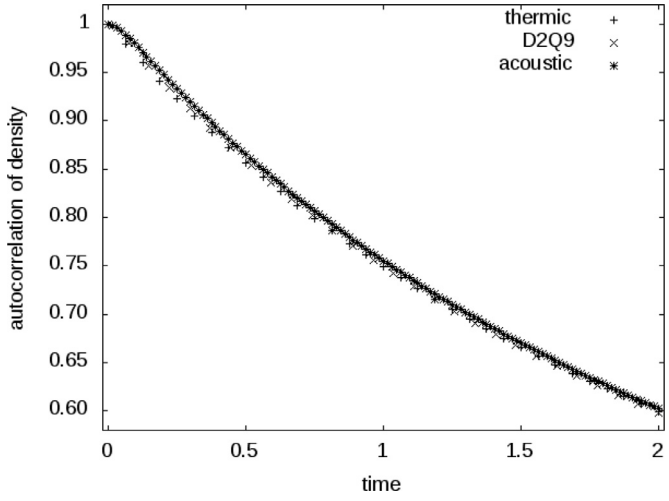

Fig. 19. Initial Gaussian, $\kappa = 0.015$. Three simulations done for the damped acoustic model with HaWAY finite differences, D2Q9 lattice Boltzmann scheme and for the heat equation with finite differences. Autocorrelation of density at time = 2 for a 27×27 mesh.

mined in such a way that the usual relation (10) is satisfied, towards the damped acoustic system. Due to the mathematical convergence of the lattice Boltzmann scheme with diffusive scaling [13], this result is unexpected, as pointed in the title.

The results presented here can be interpreted physically in terms of frequency dependent transport coefficients that should be used when the time scale of the macroscopic phenomenon under study is not very large compared to microscopic time scales. Future study should focus on the extension of this analysis to second order. A natural extension of this question concerns lattice Boltzmann models conserving *a priori* both mass and momentum. Our preliminary results show that a system of five partial differential equations is emergent in the case of two space dimensions. This question will be studied in a forthcoming contribution.

Acknowledgments

The authors thank the Fondation Mathématique Jacques Hadamard for funding our collaboration. This work is also partially supported by the French “Climb” Oseo project. Las but not least,

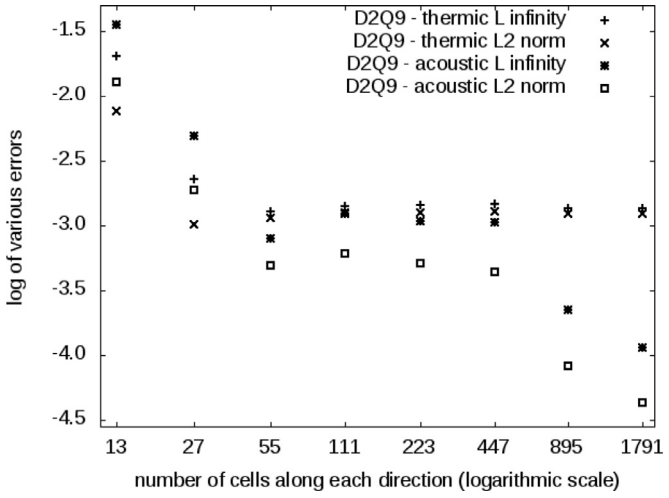

Fig. 20. Initial Gaussian, $\kappa = 0.015$. Three simulations done for the damped acoustic model with finite differences HaWAY discretization, D2Q9 lattice Boltzmann scheme and for the heat equation with finite differences. The order of convergence at time = 2 towards damped acoustic is 0.954 for the L^2 norm and 0.934 in norm L^∞.

the authors thank the referees for their precise comments on the first draft of this contribution.

Appendix

A1. HaWAY staggered finite differences

We consider the acoustic model proposed in Eq. (38):

$$\begin{cases} \dfrac{\partial \rho}{\partial t} + \dfrac{\partial J^x}{\partial x} + \dfrac{\partial J^y}{\partial y} = 0 \\ \dfrac{\partial J^x}{\partial t} + c_0^2 \dfrac{\partial \rho}{\partial x} + g J^x = 0 \\ \dfrac{\partial J^y}{\partial t} + c_0^2 \dfrac{\partial \rho}{\partial y} + g J^y = 0. \end{cases} \tag{46}$$

Given a spatial grid Δx, Δy and a time step Δt, we consider integer multiples of these parameters for the discretization in space and time. The density ρ is approximated at half-integer vertices in space and integer points in time whereas the momentum J^x (respectively J^y) is approximated at integer nodes (respectively half-integer nodes) in the x-direction, semi-integer nodes (respectively integer nodes) in the y-direction, and half-integer values in time:

$$\rho \approx \rho^n_{i+1/2,j+1/2}, \quad J^x \approx J^{x,n+1/2}_{i,j+1/2}, \quad J^y \approx J^{y,n+1/2}_{i+1/2,j}. \tag{47}$$

The Fig. A.21 gives an illustration of this classical choice [1,8,18].

- We discretize the first equation of Eq. (46) with a four-point centered finite-difference schemes around the vertex $\left((i+\frac{1}{2})\Delta x, (j+\frac{1}{2})\Delta y, (n+\frac{1}{2})\Delta t\right)$:

$$\begin{cases} \dfrac{\rho^{n+1}_{i+1/2,j+1/2} - \rho^n_{i+1/2,j+1/2}}{\Delta t} + \dfrac{J^{x,n+1/2}_{i+1,j+1/2} - J^{x,n+1/2}_{i,j+1/2}}{\Delta x} \\ + \dfrac{J^{y,n+1/2}_{i+1/2,j+1} - J^{y,n+1/2}_{i+1/2,j}}{\Delta y} = 0. \end{cases} \tag{48}$$

We use the same approach for the discretization of the second equation of Eq. (46) around the node $\left(i\Delta x, (j+\frac{1}{2})\Delta y, n\Delta t\right)$:

$$\frac{J^{x,n+1/2}_{i,j+1/2} - J^{x,n-1/2}_{i,j+1/2}}{\Delta t} + \frac{c_0^2}{\Delta x}\left(\rho^n_{i+1/2,j+1/2} - \rho^n_{i-1/2,j+1/2}\right) + g J^{x,n}_{i,j+1/2} = 0 \tag{49}$$

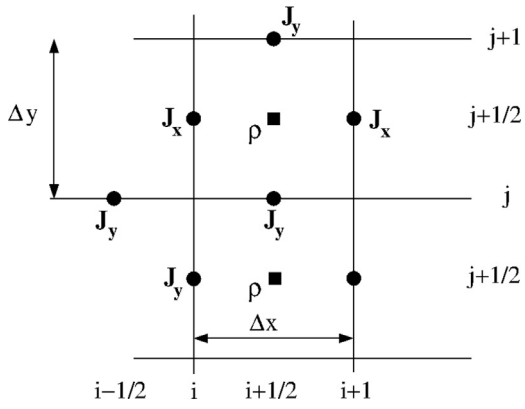

Fig. A1. HaWAY grid for staggered (density, momentum) finite differences.

and the third equation of Eq. (46) around the node $\left((i+\frac{1}{2})\Delta x, j\Delta y, n\Delta t\right)$:

$$\frac{J^{y,n+1/2}_{i+1/2,j}-J^{y,n-1/2}_{i+1/2,j}}{\Delta t}+\frac{c_0^2}{\Delta y}\left(\rho^n_{i+1/2,j+1/2}-\rho^n_{i+1/2,j-1/2}\right)+gJ^{y,n}_{i+1/2,j}=0. \tag{50}$$

We interpolate the momentum at integer time vertices with a simple average:

$$J^{x,n}_{i,j+1/2}=\frac{1}{2}\left(J^{x,n+1/2}_{i,j+1/2}+J^{x,n-1/2}_{i,j+1/2}\right), J^{y,n}_{i+1/2,j}=\frac{1}{2}\left(J^{y,n+1/2}_{i+1/2,j}+J^{y,n-1/2}_{i+1/2,j}\right).$$

We incorporate these expressions into the relations Eqs. (49) and (50). We obtain

$$\begin{cases}\left(\frac{1}{\Delta t}+\frac{g}{2}\right)J^{x,n+1/2}_{i,j+1/2}+\frac{c_0^2}{\Delta x}\left(\rho^n_{i+1/2,j+1/2}-\rho^n_{i-1/2,j+1/2}\right)\\ \qquad=\left(\frac{1}{\Delta t}-\frac{g}{2}\right)J^{x,n-1/2}_{i,j+1/2}\end{cases} \tag{51}$$

and

$$\begin{cases}\left(\frac{1}{\Delta t}+\frac{g}{2}\right)J^{y,n+1/2}_{i+1/2,j}+\frac{c_0^2}{\Delta y}\left(\rho^n_{i+1/2,j+1/2}-\rho^n_{i+1/2,j-1/2}\right)\\ \qquad=\left(\frac{1}{\Delta t}-\frac{g}{2}\right)J^{y,n-1/2}_{i+1/2,j}.\end{cases} \tag{52}$$

The numerical scheme is now entirely defined for internal nodes. In this study we have used periodic boundary conditions.

References

[1] Arakawa A. Computational design for long-term numerical integration of the equations of fluid motion. J Comput Phys 1966;1:119–43.
[2] Augier A, Graille B, Dubois F. On rotational invariance of lattice Boltzmann schemes. Comput Math Appl 2014;67:239–55.
[3] Boghosian B, Dubois F, Graille B, Lallemand P, Tekitek M. Curious convergence properties of lattice Boltzmann schemes for diffusion with acoustic scaling. Commun Comput Phys 2018.
[4] Dellacherie S. Construction and analysis of lattice Boltzmann methods applied to a 1d convection-diffusion equation. Acta Applicandae Mathematica 2014;131(1):69–140.
[5] Dubois F. Third order equivalent equation of lattice Boltzmann scheme. Discrete Continuous Dyn Syst 2009;23:221–48.
[6] Dubois F, Lallemand P. Towards higher order lattice Boltzmann schemes. J Stat Mech 2009:P06006.
[7] Dubois F, Lallemand P. On triangular lattice Boltzmann schemes for scalar problems. Commun Comput Phys 2013;13:649–70.
[8] Harlaw FH, Welsch JE. Numerical calculation of time-dependent viscous incompressible flow of fluid with a free surface. Phys Fluids 1965;8:2182–9.
[9] Hénon M. Viscosity of a lattice gas. Complex Syst 1987;1:763–89.
[10] d'Humières D. Generalized lattice-Boltzmann equations in rarefied gas dynamics: theory and simulations. AIAA Prog Astronaut Astronaut 1992;159:450–8.
[11] Junk M, Klar A, Luo LS. Asymptotic analysis of the lattice Boltzmann equation. J Comput Phys 2005;210:676–704.
[12] Junk M, Yang Z. Convergence of lattice Boltzmann methods for Navier–Stokes flows in periodic and bounded domains. Numerische Mathematik 2009;112(1):65–87.
[13] Junk M, Yang Z. l^2 convergence of the lattice Boltzmann method for one dimensional convection-diffusion-reaction equations. Commun Comput Phys 2015;17(5):1225–45.
[14] Lallemand P, d'Humières D, Luo LS, Rubinstein R. Theory of the lattice Boltzmann method: three-dimensional model for linear viscoelastic fluids. Phys Rev E 2003;67:021203.
[15] Lallemand P, Luo LS. Theory of the lattice Boltzmann method: dispersion, dissipation, isotropy, galilean invariance, and stability. Phys Rev E 2000;61:6546–62.
[16] Pinsky M. Differential equations with a small parameter and the central limit theorem for functions defined on a finite Markov chain. Z Wahrscheinlichkeitstheorie und Verw Gebiete 9 1968;9(2):101–11.
[17] Richtmyer RD, Morton KW. Difference methods for initial-value problems. New York: Interscience Publishers; 1957.
[18] Yee K. Numerical solution of initial boundary value problems involving Maxwell's equations in isotropic media. IEEE Trans Antennas Propag 1966;14:302–7.